The current issue and full text archive of this journal is available at
www.emeraldinsight.com/0961-5539.htm

Pressure drop caused by two-phase flow of oil/water emulsions through sudden expansions and contractions: a computational approach

Received 5 October 2007
Revised 13 June 2008
Accepted 12 August 2008

Manmatha K. Roul and Sukanta K. Dash
Department of Mechanical Engineering, Indian Institute of Technology, Kharagpur, India

Abstract

Purpose – The purpose of this paper is to compute the pressure drop through sudden expansions and contractions for two-phase flow of oil/water emulsions.

Design/methodology/approach – Two-phase computational fluid dynamics (CFD) calculations, using Eulerian–Eulerian model, are employed to calculate the velocity profiles and pressure drops across sudden expansions and contractions. The pressure losses are determined by extrapolating the computed pressure profiles upstream and downstream of the expansion/contraction. The oil concentration is varied over a wide range of 0-97.3 percent by volume. The flow field is assumed to be axisymmetric and solved in two dimensions. The two-dimensional equations of mass, momentum, volume fraction and turbulent quantities along with the boundary conditions have been integrated over a control volume and the subsequent equations have been discretized over the control volume using a finite volume technique to yield algebraic equations which are solved in an iterative manner for each time step. The realizable per phase k-ε turbulent model is considered to update the fluid viscosity with iterations and capture the individual turbulence in both the phases.

Findings – The contraction and expansion loss coefficients are obtained from the pressure loss and velocity data for different concentrations of oil–water emulsions. The loss coefficients for the emulsions are found to be independent of the concentration and type of emulsions. The numerical results are validated against experimental data from the literature and are found to be in good agreement.

Research limitations/implications – The present computation could not use the surface tension forces and the energy equation due to huge computing time requirement.

Practical implications – The present computation could compute realistically the two-phase pressure drop through sudden expansions and contractions by using a two-phase Eulerian model and hence this model can be effectively used for industrial applications where two-phase flow comes into picture.

Originality/value – The original contribution of the paper is in the use of the state-of-the-art Eulerian two-phase flow model to predict the velocity profile and pressure drop through industrial piping systems.

Keywords Flow, Pressure, Velocity measurement, Concentration, Emulsions
Paper type Research paper

Nomenclature

C_c = coefficient of contraction
C_D = drag coefficient
C_L = lift coefficient
C_{VM} = virtual mass coefficient
D_1 = inlet pipe diameter
D_2 = outlet pipe diameter
d = diameter of bubble (m)
G = production of turbulent kinetic energy
$\vec{g}$ = acceleration due to gravity (m/s^2)

International Journal of Numerical Methods for Heat & Fluid Flow
Vol. 19 No. 5, 2009
pp. 665-688

0961-5539
DOI 10.1108/09615530910963580

K = loss coefficient
k = turbulent kinetic energy
M = interfacial forces
M^d = drag force
M^L = lift force
M^{VM} = virtual mass force
ΔP = pressure drop
ΔP_e = pressure drop through expansion
ΔP_c = pressure drop through contraction
Re = Reynolds number

Greek symbols

α = volume fraction
ε = dissipation rate of turbulent kinetic energy
μ = viscosity (kg/ms)
μ_t = turbulent viscosity
μ^{eff} = effective viscosity
ρ = density (kg/m^3)
σ_k = turbulent Prandtl number for k
σ_ε = turbulent Prandtl number for ε
$\bar{\bar{\tau}}$ = stress tensor
$\vec{v}$ = velocity vector

Subscripts

C = vena-contracta
c = contraction
e = expansion
p = secondary phase
q = primary phase

1. Introduction

Modification of flow due to a sudden change in the pipe diameter gives rise to additional pressure drop along the flow path. Knowledge of this additional pressure drop is extremely important for a proper assessment of the pumping power required in pipes. In contrast to the well-known axial pressure profiles in the transitional region between the flow separation and reattachment for single-phase liquid flow, the pressure profiles and the shape of streamlines in two-phase flow are still unknown. Due to inherent complexity of two-phase flows through such sections, from a physical as well as numerical point of view, generally applicable computational fluid dynamics (CFD) codes are non-existent. Two-phase flow of oil/water emulsions find application in a number of industries, such as petroleum, pharmaceutical, agriculture and food industries etc. In many applications, pumping of emulsions through pipes and pipe fittings is required. Since a detailed physical description of the flow mechanism is still not possible for two-phase flow, a considerable effort is generally needed to calculate the pressure drop along the flow path.

Several papers have been published on flow of two-phase gas/liquid and liquid/liquid mixtures through pipe fittings. Hwang and Pal (1997) studied experimentally the flow of oil/water emulsions through sudden expansions and contractions and found that the loss coefficient for emulsions is independent of the concentration and type of emulsions. Schmidt and Friedel (1997) also studied experimentally two-phase pressure drop across sudden contractions using mixtures of air and liquids, such as water, aqueous glycerol, calcium nitrate solution and refrigerant R_{12} in dependence of the most relevant physical parameters and concluded that unlike single phase flow a two-phase flow does not contract behind the edge of transition. They also reported that the contraction coefficient is not a physically reasonable parameter in two-phase flow and therefore should not be used as intermediate parameter to calculate the two-phase pressure drop. Wadle (1989) carried out a theoretical and experimental study on the pressure recovery in abrupt expansions. He proposed a formula for the pressure recovery based on the superficial velocities of the

two phases and verified its predictive accuracy with measured experimental steam-water and air-water data. Tapucu *et al.* (1989) observed that emulsions can be treated as pseudo-homogeneous fluids with suitably averaged properties as the dispersed droplets of emulsions are small and are well dispersed. Consequently, the pressure loss for emulsion flow in expansion and contraction should be determinable in the same way as for single-phase fluid flow. Acrivos and Schrader (1982) observed that significant velocity slip occurs at both sides of the enlargement for two-phase flow mixtures. Attou *et al.* (1997) developed a semi-analytical model for two-phase pressure drop in sudden enlargements, based on the solution of one-dimensional conservation equations downstream of the enlargement. They compared the predictions of three models (homogeneous flow; frozen flow and bubbly flow) with experimental data, with the latter model providing the best agreement with data. Two-phase flow across sudden contractions is considerably more complicated than sudden enlargements. Many of the published studies have assumed the occurrence of the vena-contracta phenomenon, in analogy with single-phase flow (Al'Ferov and Shul'Zhenko, 1977; Attou and Bolle, 1995; Gnglielmini *et al.*, 1986; Jansen, 1966) and have assumed that dissipation occurs downstream of the vena-contracta point. The above and other models which are based on vena-contracta phenomenon, generally assume that for a particular system the vena-contracta in single-phase and two-phase flows take place in the same location, and result in identical contraction ratio, Cc. Consequently, Cc is usually found from single-phase flow data. However, Schmidt and Friedel (1997) performed experiments and showed that the vena-contracta phenomenon in two-phase flow did not occur in their system at all. Abdelall *et al.* (2005) studied the pressure drop caused by abrupt flow area expansion and contraction in small channels and developed an empirical correlation for two-phase flow pressure drop through sudden area contraction. They indicated a significant velocity slip at the vicinity of the change of flow area. Salcudean *et al.* (1983) studied the effect of various flow obstructions on pressure drops in horizontal air-water flow and derived pressure loss coefficients and two-phase multipliers.

Flow in a symmetric channel with a sudden expansion makes a transition from a symmetric flow to an asymmetric one due to a symmetry-breaking bifurcation for a gradual increase of the Reynolds number in a single phase flow (Mizushima and Shiotani, 2000). In contrast to single-phase flow, the axial velocity profiles in different sections are symmetrical about the axis of the expansion in two-phase flow (Aloui and Souhar, 1996a, b) and as a result of this symmetry; 2D-axisymmetric set up is considered. The objective of the present work is to simulate the flow of oil–water emulsions through sudden expansions and contractions in pipes numerically by using two-phase flow models in an Eulerian scheme. Before, we can rely on CFD models to study the fluid flow; we need to establish whether the model yields valid results. For the validation of results, we have referred to the experimental studies conducted by Hwang and Pal (1997), who measured pressure drop together with spatial distributions of velocity field in oil/water two-phase flow. The realizable per-phase $k-\varepsilon$ model (Shih *et al.*, 1995) has been used as closure model for turbulent flow. This is a modified version of $k-\varepsilon$ model which correctly predicts the flow in round jets, and is also well suited for swirling flows and flows involving separation (Shih *et al.*, 1995). Although RSM turbulence model, predict the pressure drop slightly better than the realizable $k-\varepsilon$ model, however, behind the accuracy of the complicated RSM model it does require much expensive computational effort compared to the realizable $k-\varepsilon$ model. The realizable $k-\varepsilon$ turbulence model still yield a reasonably good prediction on pressure drop with deviation of less than 5 percent on measured value at different inlet velocity. Comparisons of numerical and experimental results are found to be in good agreement by employing the two-phase flow model in an Eulerian scheme.

2. Governing equations

Here we considered the two-fluid or Euler–Euler technique. In the Euler–Euler approach, the different phases are treated mathematically as interpenetrating continua, with each computational cell of the domain containing respective fractions of the continuous and dispersed phases. We have adopted the following assumptions in our study which are very realistic for the present situation.

- The fluids in both phases are Newtonian, viscous and incompressible.
- The physical properties remain constant.
- No mass transfer between the two phases.
- The pressure is assumed to be common to both the phases.
- The realizable k-ε turbulent model is applied to describe the behavior of each phase.
- The surface tension forces are neglected, therefore, the pressure of both phases are equal at any cross-section.
- The flow is assumed to be isothermal, so the energy equations are not needed.

With all the above assumptions, the governing equations for phase q can be written as (Anglart *et al.*, 1997; Crowe *et al.*, 1998; Daniel and Loraud, 1998; Drew, 1983; Drew and Lahey 1979; Drew and Passman 1999; Ranade, 2002):
Continuity equation:

$$\frac{\partial}{\partial t}(\alpha_q \rho_q) + \nabla \cdot (\alpha_q \rho_q \vec{v}_q) = 0 \tag{1}$$

The volume fractions are assumed to be continuous functions of space and time and their sum is equal to one.

$$\alpha_q + \alpha_p = 1 \tag{2}$$

Momentum equation:

$$\frac{\partial}{\partial t}(\alpha_q \rho_q \vec{v}_q) + \nabla \cdot (\alpha_q \rho_q \vec{v}_q \vec{v}_q) = -\alpha_q \nabla p + \nabla \cdot (\bar{\bar{\tau}}_q) + \alpha_q \rho_q \vec{g} + M_q \tag{3}$$

$\bar{\bar{\tau}}_q$, is the qth phase stress tensor

$$\bar{\bar{\tau}}_q = \alpha_q \mu_q^{eff} \left(\nabla \vec{v}_q + \nabla \vec{v}_q^T \right) \tag{4}$$

$$\mu_q^{eff} = \mu_q + \mu_{t,q} \tag{5}$$

where M_q is the interfacial momentum transfer term, which is given by:

$$M_q = M_q^d + M_q^{VM} + M_q^L \tag{6}$$

where the individual terms on the right-hand side of Equation (6) are, respectively, the drag force, virtual mass force and lift force. The drag force is expressed as,

$$M_q^d = \frac{3}{4d_p}\alpha_p\rho_q C_D|\vec{v}_p - \vec{v}_q|(\vec{v}_p - \vec{v}_q) \tag{7}$$

The drag coefficient C_D depends on the particle Reynolds number as given below (Gidaspow, 1994; Kishan and Dash, 2006; Wallis, 1969):

$$\begin{aligned} \mathrm{C_D} &= 24(1 + 0.15\mathrm{Re}^{0.687})/\mathrm{Re}, \quad \mathrm{Re} \le 1000 \\ &= 0.44, \qquad\qquad\qquad\quad \mathrm{Re} > 1000 \end{aligned} \tag{8}$$

Relative Reynolds number for primary phase q and secondary phase p is given by

$$\mathrm{Re} = \frac{\rho_q|\vec{v}_q - \vec{v}_p|d_p}{\mu_q} \tag{9}$$

Equation (7) shows that the drag force exerted by the secondary phase (bubbles or droplet) on the primary phase is a vector directed along the relative velocity of the secondary phase. We have varied the diameter of the particle from 10 to 100 micron and have not seen any change in the pressure profile at the expansion or contraction section.

The second term in Equation (6) represents the virtual mass force, which comes into play when one phase is accelerating relative to the other one. In case of bubble or droplet accelerating in a continuous phase, this force can be described by the following expression (Anglart *et al.*, 1997; Drew, 1983; Kishan and Dash, 2006):

$$M_q^{VM} = -M_p^{VM} = C_{VM}\alpha_p\rho_q\left(\frac{d_q\vec{v}_q}{dt} - \frac{d_p\vec{v}_p}{dt}\right) \tag{10}$$

where C_{VM} is the virtual mass coefficient, which for a spherical particle is equal to 0.5. (Drew, 1983).

The third term in Equation (6) is the lift force, which arises from a velocity gradient of the continuous phase in the lateral direction and is given by (Anglart *et al.*, 1997; Drew and Lahey, 1979).

$$M_q^L = -M_p^L = C_L\alpha_p\rho_q(\vec{v}_p - \vec{v}_q) \times (\nabla \times \vec{v}_q) \tag{11}$$

where C_L is the lift force coefficient, which for shear flow around a spherical droplet is equal to 0.5.

2.1 Turbulence modeling

Here we considered the realizable per-phase $k - \varepsilon$ turbulence model (Shih *et al.*, 1995; Launder and Spalding, 1974; Troshko and Hassan, 2001).

Transport equations for k:

$$\begin{aligned} &\frac{\partial}{\partial t}(\alpha_q\rho_q k_q) + \nabla\cdot\left(\alpha_q\rho_q\overrightarrow{U}_q k_q\right) = \nabla\cdot\left[\alpha_q\left(\mu_q + \frac{\mu_{t,q}}{\sigma_k}\right)\nabla k_q\right] + \left(\alpha_q G_{k,q} - \alpha_q\rho_q\varepsilon_q\right) \\ &+ K_{pq}(C_{pq}k_p - C_{qp}k_q) - K_{pq}(\overrightarrow{U}_p - \overrightarrow{U}_q)\cdot\frac{\mu_{t,p}}{\alpha_p\sigma_p}\nabla\alpha_p + K_{pq}(\overrightarrow{U}_p - \overrightarrow{U}_q)\cdot\frac{\mu_{t,q}}{\alpha_q\sigma_q}\nabla\alpha_q \end{aligned} \tag{12}$$

Transport equations for ε:

$$\frac{\partial}{\partial t}(\alpha_q\rho_q\varepsilon_q)+\nabla\cdot(\alpha_q\rho_q\vec{U}_q\varepsilon_q)=\nabla\cdot\left[\alpha_q\left(\mu_q+\frac{\mu_{t,q}}{\sigma_\varepsilon}\right)\nabla\varepsilon_q\right]$$
$$+\alpha_q\rho_qC_1S\varepsilon_q-C_2\alpha_q\rho_q\frac{\varepsilon_q^2}{k_q+\sqrt{\nu_{t,q}\varepsilon_q}}$$
$$+C_{1\varepsilon}\frac{\varepsilon_q}{k_q}\left[K_{pq}(C_{pq}k_p-C_{qp}k_q)-K_{pq}(\vec{U}_p-\vec{U}_q)\right.$$
$$\left.\cdot\frac{\mu_{t,p}}{\alpha_p\sigma_p}\nabla\alpha_p+K_{pq}(\vec{U}_p-\vec{U}_q)\cdot\frac{\mu_{t,q}}{\alpha_q\sigma_q}\nabla\alpha_q\right] \quad (13)$$

where, $\vec{U}_q$ is the phase-weighted velocity. Here,

$$C_1=\max\left[0.43,\frac{\eta}{\eta+5}\right],\eta=S\frac{k}{\varepsilon},S=(2S_{ij}S_{ij})^{0.5}$$

The terms C_{pq} and C_{qp} can be approximated as

$$C_{pq}=2,C_{qp}=2\left(\frac{\eta_{pq}}{1+\eta_{pq}}\right) \quad (14)$$

where η_{pq} is defined as

$$\eta_{pq}=\frac{\tau_{t,pq}}{\tau_{F,pq}} \quad (15)$$

where, the Langrangian integral time scale $(\tau_{t,pq})$, is defined as

$$\tau_{t,pq}=\frac{\tau_{t,q}}{\sqrt{(1+C_\beta\xi^2)}} \quad (16)$$

where,

$$\xi=\frac{|\vec{v}_{pq}|\tau_{t,q}}{L_{t,q}} \quad (17)$$

where $\tau_{t,q}$ is a characteristic time of the energetic turbulent eddies and is defined as:

$$\tau_{t,q}=\frac{3}{2}C_\mu\frac{k_q}{\varepsilon_q} \quad (18)$$

and

$$C_\beta=1.8-1.35\cos^2\theta \quad (19)$$

where, θ is the angle between the mean particle velocity and the mean relative velocity. The characteristic particle relaxation time connected with inertial effects acting on a dispersed phase p is defined as

$$\tau_{F,pq} = \alpha_p \rho_q K_{pq}^{-1} \left(\frac{\rho_p}{\rho_q} + C_V \right) \tag{20}$$

where, $C_V = 0.5$.

The eddy viscosity model is used to calculate averaged fluctuating quantities. The Reynolds stress tensor for continuous phase q is given as:

$$\bar{\bar{\tau}}_q = -\frac{2}{3}(\rho_q k_q + \rho_q \mu_{t,q} \nabla \cdot \vec{U}_q)\bar{\bar{I}} + \rho_q \mu_{t,q}(\nabla \vec{U}_q + \nabla \vec{U}_q^T) \tag{21}$$

The turbulent viscosity $\mu_{t,q}$ is written in terms of the turbulent kinetic energy of phase q:

$$\mu_{t,q} = \rho_q C_\mu \frac{k_q^2}{\varepsilon_q} \tag{22}$$

The production of turbulent kinetic energy, $G_{k,q}$ is computed from

$$G_{k,q} = \mu_{t,q}(\nabla \vec{v}_q + \nabla \vec{v}_q^T) : \nabla \vec{v}_q \tag{23}$$

The production term in the ε equation (the second term on the right-hand side of Equation (28) does not contain the same G_k term as the other $k - \varepsilon$ models. Another desirable feature in the realizable $k - \varepsilon$ model is that the destruction term [(the third term on right-hand side of Equation (28)] does not have any singularity i.e. its denominator never vanishes, even if k vanishes or become smaller than zero. This feature is contrasted with traditional $k - \varepsilon$ models, which have a singularity due to k in denominator. Unlike standard and RNG $k - \varepsilon$ models, C_μ is not a constant here. It is computed from:

$$C_\mu = \frac{1}{A_0 + A_s \frac{kU^*}{\varepsilon}} \tag{24}$$

where

$$U^* \equiv \sqrt{S_{ij} S_{ij} + \tilde{\Omega}_{ij} \tilde{\Omega}_{ij}} \tag{25}$$

and

$$\tilde{\Omega}_{ij} = \Omega_{ij} - 2\varepsilon_{ijk}\omega_k$$
$$\Omega_{ij} = \overline{\Omega_{ij}} - \varepsilon_{ijk}\omega_k$$

where, $\overline{\Omega_{ij}}$ is the mean rate of rotation tensor viewed in a rotating reference frame with the angular velocity $\overline{\omega_k}$. The constants A_0 and A_s are given by

$$A_0 = 4.04, A_s = \sqrt{6}\cos\phi$$

where

$$\phi = \frac{1}{3}\cos^{-1}(\sqrt{6}W), W = \frac{S_{ij}S_{jk}S_{ki}}{S^3}, \tilde{S} = \sqrt{S_{ij}S_{ij}}, S_{ij} = \frac{1}{2}\left(\frac{\partial u_j}{\partial x_i} + \frac{\partial u_i}{\partial x_j}\right)$$

The constants used in the model are the following:

$$C_{1\varepsilon} = 1.44; C_2 = 1.9; \sigma_k = 1.0; \sigma_\varepsilon = 1.2.$$

Inter-phase turbulent momentum transfer:

The turbulent drag term $K_{pq}(\vec{v}_p - \vec{v}_q)$ is modeled as follows:

$$K_{pq}(\vec{v}_p - \vec{v}_q) = K_{pq}\left(\overrightarrow{U}p - \overrightarrow{U}q\right) - K_{pq}\vec{v}_{dr,pq} \tag{26}$$

Here $\overrightarrow{U}_p$ and $\overrightarrow{U}_q$ are phase-weighted velocities, and $\vec{v}_{dr,pq}$ is the drift velocity for phase p, which is computed as follows:

$$\vec{v}_{dr,pq} = -\left(\frac{D_p}{\sigma_{pq}\alpha_p}\nabla\alpha_p - \frac{D_q}{\sigma_{pq}\alpha_q}\nabla\alpha_q\right) \tag{27}$$

The diffusivities D_p and D_q are computed directly from the transport equations. The drift velocity results from turbulent fluctuations in the volume fraction. When multiplied by the exchange coefficient K_{pq}, it serves as a correction to the momentum exchange term for turbulent flows.

2.2 Boundary conditions

Velocity inlet boundary condition is applied at the inlet (as can be seen from Figure 1). A no-slip and no-penetrating boundary condition is imposed on the wall of the pipe. At the outlet, the boundary condition is assigned as outflow, which implies diffusion flux for the entire variables in exit direction are zero. Symmetry boundary condition is

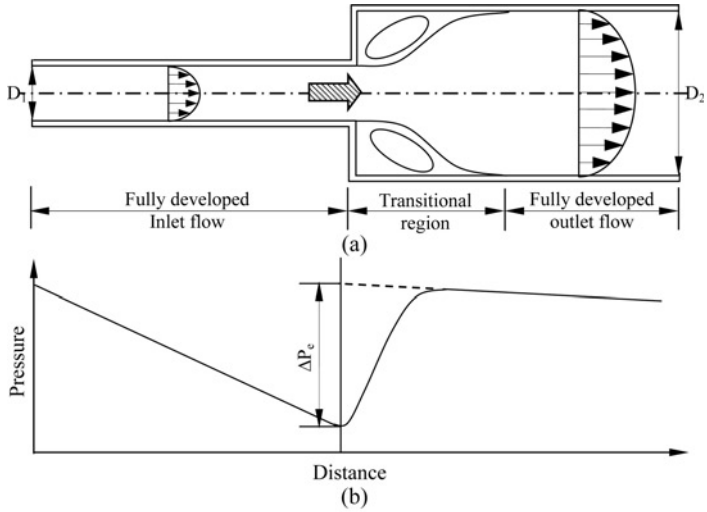

Figure 1.

Notes: (a) Idealized course of boundary stream lines and (b) pressure profile for a sudden expansion

considered at the axis, which implies normal gradients of all flow variables are zero and radial velocity is zero at the axis.

3. Numerical solution procedures

The objective of the present work is to simulate the flow through sudden contraction and expansion in pipes numerically by using two-phase flow models in an Eulerian scheme. The flow field is assumed to be axisymmetric and solved in two dimensions. The two-dimensional equations of mass, momentum, volume fraction and turbulent quantities along with the boundary conditions have been integrated over a control volume and the subsequent equations have been discretized over the control volume using a finite volume technique to yield algebraic equations which are solved in an iterative manner for each time step. The finite difference algebraic equations for the conservation equations are solved using Fluent6.2 (2005) double precision solver with an implicit scheme for all variables with a final time step of 0.001 for quick convergence. The discretization form for all the convective variables are taken to be first order up winding initially for better convergence. Slowly as time progressed the discretization forms are switched over to second order up winding and then slowly towards the QUICK scheme for better accuracy. The Phase-Coupled SIMPLE algorithm(Vasquez and Ivanov, 2000) which is an extension of the SIMPLE algorithm (Patankar, 1980) for multiphase flows is used for the pressure-velocity coupling. The velocities are solved coupled by the phases, but in a segregated fashion. The block algebraic multigrid scheme is used to solve a vector equation formed by the velocity components of all phases simultaneously. Pressure and velocities are then corrected so as to satisfy the continuity constraint. The realizable per-phase k-ε model (Shih *et al.*, 1995) has been used as closure model for turbulent flow. Fine grids are used near the wall as well as near the contraction and expansion section to capture more details of velocity and volume fraction changes.

4. Theoretical background

Figure 2 shows a cross-section of the test section. At this section there is a sudden, sharp edged contraction (or expansion, depending upon the flow direction). Figure 2(a)

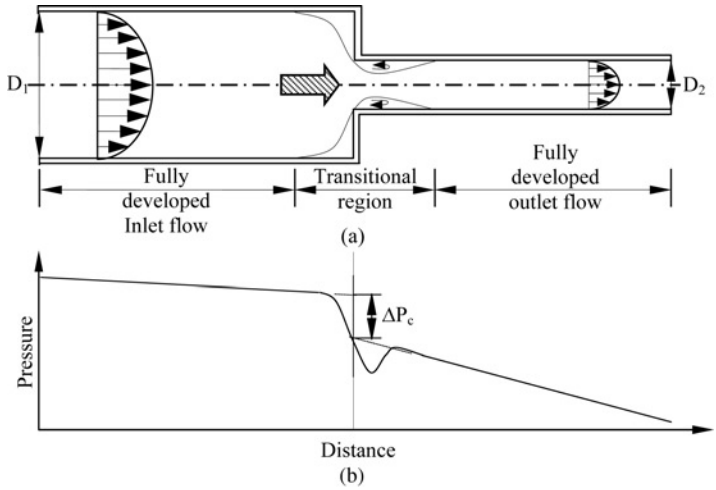

Notes: (a) Idealized course of boundary stream lines and (b) pressure profile for a sudden contraction

Figure 2.

shows the schematic diagram of the boundary streamlines for the flow through a sudden contraction, while Figure 2(b) depicts the graph of the static pressure along the flow axis for a steady-state flow of an incompressible fluid across a contraction. This conception is based on measurements in single-phase flow of water through sudden contractions (Schmidt and Friedel, 1997). In a distance of about 1.5 times the entrance-pipe diameter in front of the transitional cross-section the flow separates from the inner wall and contracts to a jet with a narrowest cross-section immediately behind the transition. Hereafter, the jet enlarges and the main flow reattaches to the pipe wall in a distance of less than 14 times the outlet-pipe diameter (Schmidt and Friedel, 1997), depending on the flow condition. The friction loss (h_f) due to a pipe contraction can be calculated from the following equation:

$$h_f = \frac{P_1 - P_2}{\rho} + K_1 \frac{V^2}{2} \tag{28}$$

where h_f is the friction loss, $(P_1 - P_2)$ is the pressure change at the contraction plane (ΔP_c), ρ is the mean fluid density, K_1 is equal to $[(D_2/D_1)^4 - 1]$ and V is the average velocity in a small diameter pipe. The pressure change at the contraction plane (ΔP_c) can be determined by extrapolating the computed pressure profiles upstream and downstream of the pipe contraction (in the region of fully developed pipe flow) to the contraction plane as has been done in the present work.

Since the flow regime is turbulent, $\Delta P_c/\rho$ vs $V^2/2$ data exhibit a linear relationship such as:

$$\frac{\Delta P_c}{\rho} = K_2 \frac{V^2}{2} \tag{29}$$

V is the average velocity in a small-diameter pipe and K_2 is the slope of $\Delta P_c/\rho$ vs $V^2/2$ plot. From Equations (28) and (29), the frictional loss (h_f) due to a pipe contraction is given by:

$$h_f = (K_1 + K_2) \frac{V^2}{2} = K_c \frac{V^2}{2} \tag{30}$$

where, the loss coefficient for contraction (K_c) is equal to$(K_1 + K_2)$.

Similarly with reference to Figure 1, the expression for the loss coefficient for expansion (K_e) can be obtained. But for sudden expansion K_1 is taken as $[1 - (D_1/D_2)^4]$.

5. Results and discussion

The sudden expansion and sudden contraction considered in this work are made from two straight pipes having inner diameters of 2.037 and 4.124 cm. Axial static pressure profiles are computed both upstream and downstream from the expansion or contraction plane. By extrapolating these pressure profiles to the contraction (or expansion) plane the pressure drop is calculated. The pressure differentials are computed with respect to the reference pressure at 25D (smaller of D_1 and D_2) upstream position. The oil used in the present computational work is Bayol-35 (Esso Petroleum, Canada), which is a refined white mineral oil with a density of 780 kg/m^3 and a

viscosity of 0.00272 Pa-s at 25 °C. Density and viscosity of water are taken as 998.2 kg/m^3 and 0.001003 Pa-s, respectively. The volume fraction of oil is taken as 0, 0.2144, 0.3886, 0.6035, 0.6457, 0.6950, 0.8042 and 0.9728. The emulsions are considered as oil-in-water (O/W) type (water is taken as the continuous phase and oil as dispersed phase) up to an oil concentration of 62 percent by volume and water-in-oil (W/O) type (oil is taken as the continuous phase and water as dispersed phase) beyond 64 percent by volume (Pal, 1993).

Figure 3 shows the domain used to represent the sudden contraction section (half of the section is modeled, with a symmetry boundary at the centerline). Calculations are performed with different mesh resolutions for one inlet velocity. The solutions of these simulations, i.e. axial pressure profiles for different mesh resolutions are compared as shown in Figure 4. From the figure, it can be seen that there are different mesh resolution in the expanded and the contracted section. The first column shows the mesh used in the expanded section and the second column shows the mesh used in the contracted section. The axial pressure profiles are plotted for different mess resolutions and compared with the experimental data for oil volume fraction of 0.2144 and inlet velocity of 6.2 m/s. The mesh resolution of 675×45 and 675×20 did not influence the final solution by more than about 3-4 percent, and hence was established as an optimal resolution and for further computations this mesh size is used in the expanded and in the contracted section. The total absolute residuals (for each variable) are scaled (scaled to the base residual value which is obtained at the first 1 or 2 iterations or mostly in the first 5 iterations, the maximum of such residual becomes the base residual) for continuity, velocity of water and oil in axial and radial directions, k and ε for water and oil, and volume fraction for oil and are monitored with iterations. The convergence criteria for all the variables are taken to be 0.001. When the scaled residuals fall below the pre assigned value of 0.001, the solution is said to have converged. A truly converged solution is one that is no longer changing with successive iteration. If the residuals for all problem variables fall below the convergence criteria but are still in decline, the solution is still changing, to a greater or lesser degree. A better indicator occurs when the residuals flatten in a traditional residual plot (of residual value vs iteration). Convergence was judged not only by examining scaled residual levels, but also by monitoring the average velocities at three different locations very close to the contraction/expansion section (at 5D upstream, at the contraction/expansion and at 5D downstream). The solution was considered to have converged when there was no further observable change in the velocity at each location.

To ensure fully developed flow before it hits the expansion/contraction section the length of the inlet section was taken sufficiently large. It had been established by taking the velocity plots in the transverse directions at different locations from inlet section as

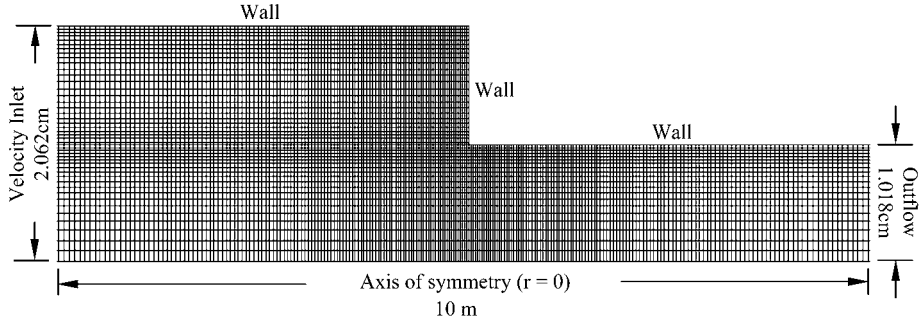

Figure 3.
Computational domain

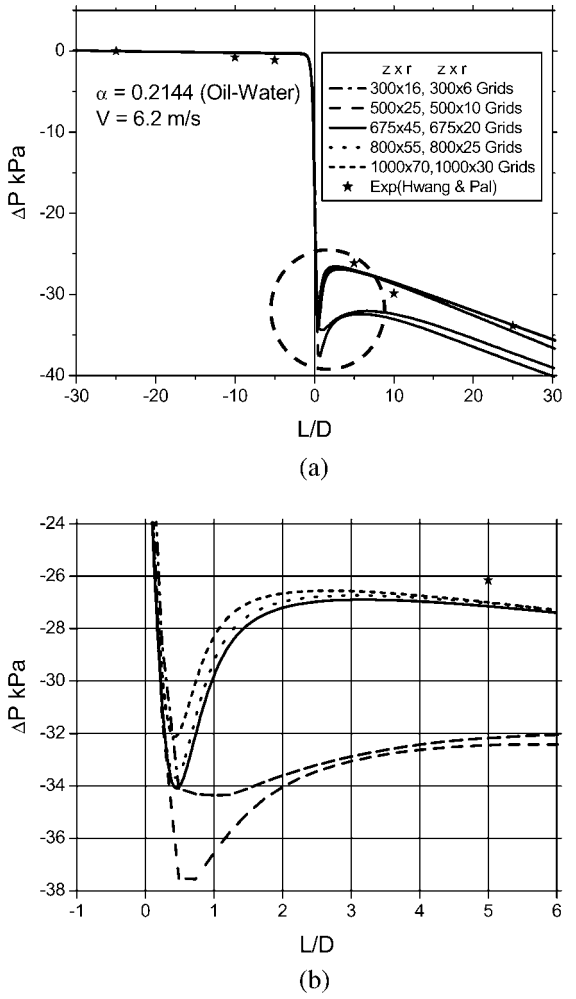

Notes: (a) Tests of Grid independence (z×r: grids in axial and radial direction before and after contraction) and (b) Magnified view of the encircled portion. — represents present case

Figure 4.

shown in Figure 5. It is evident from the plot that there is no change in velocity profile after 1 m from the inlet section. The length of the larger and smaller diameter pipe was taken to be 5 m each.

The standard $k-\varepsilon$ model is not recommended for highly swirling flows, round jets, or for flows with strong flow separation, but the realizable $k-\varepsilon$ model, which is a modified version of $k-\varepsilon$ model correctly predicts the flow in round jets, and is also well suited for swirling flows and flows involving separation (Shih *et al.*, 1995). The RSM model did not make a significant difference on the pressure distribution prediction as can be seen from the Figure 6, where the axial pressure profiles predicted by standard $k-\varepsilon$ model, realizable $k-\varepsilon$ model and RSM model are shown and compared with the experimental data (Hwang and Pal, 1997). However, RSM model is

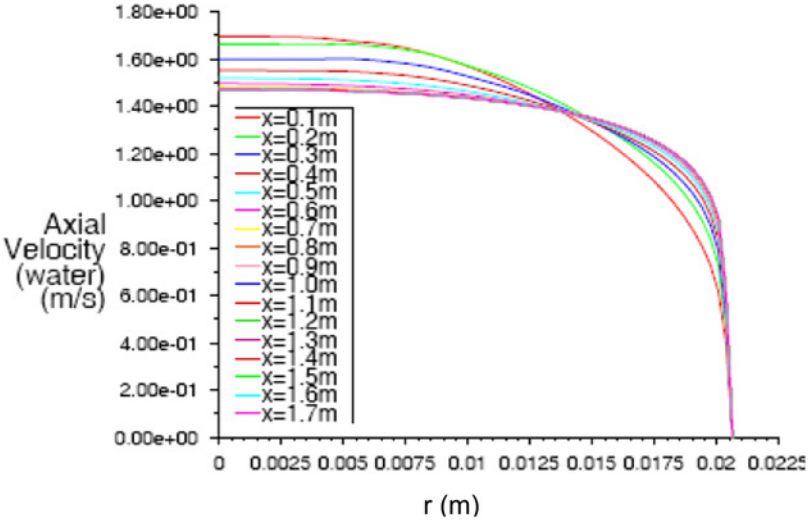

Figure 5.
Axial velocity at different transverse sections for $\alpha = 0.2144$ and v = 5.3 m/s (small diameter pipe) for flow through sudden contraction, showing a condition of fully developed flow

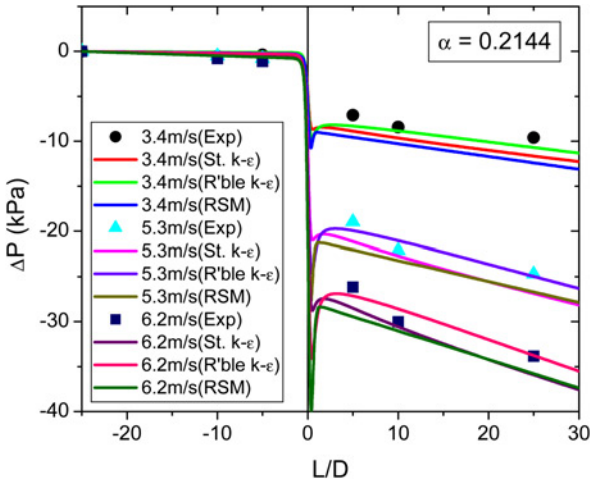

Figure 6.
Axial pressure profiles for different inlet velocities with many different turbulence models

more complicated and it requires much expensive computational effort compared to the realizable $k - \varepsilon$ model. The realizable $k - \varepsilon$ turbulence model yielded a reasonably good prediction on pressure drop with deviation of less than 5 percent from measured values at different inlet velocities.

5.1 Sudden contraction

The pressure drop across a pipe contraction (ΔP_c) is defined as a local change of pressure in the contraction plane for an assumed fully developed flow in the inlet and the outlet pipes. Computed as well as experimental pressure profiles (Hwang and Pal, 1997) for oil-in-water emulsions at various fluid velocities and concentrations are shown in Figure 7. It can be seen that the pressure profiles are nearly linear up to 5 pipe diameters, both upstream and downstream from the contraction plane. Because there is a change in pipe cross-section and hence a change in mean velocity, the slopes of the

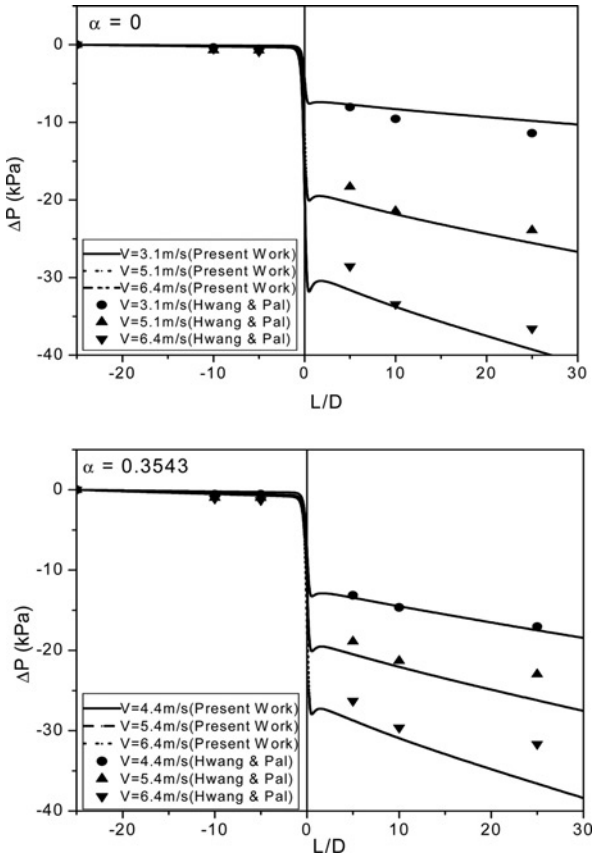

Figure 7.
Pressure profile for oil-in-water emulsion flowing through sudden contraction

pressure profiles before and after the contraction are different. The gradients are greater in the smaller diameter pipe.

The pressure profiles for the water-in-oil emulsions are shown in Figure 8. The water-in-oil emulsions behave in a manner similar to the oil-in-water emulsions. From both Figures 7 and 8, it can be seen that there is a fairly good agreement between the present computation and that of the experimental observation for the pressure drop in the sudden contraction.

It can be observed from Figures 7 and 8 that very close to the contraction plane the static pressure in the inlet line decreases more rapidly than in fully developed flow region. It attains the (locally) smallest value at a distance of about 10 mm (L/D = 0.5) after the contraction section and depends only slightly on the concentration and inlet velocity of flow.

This phenomenon is clearly indicated in Figure 9, which is an enlarged view of Figure 7 (for $\alpha = 0.3886$). The same is also demonstrated by the streamline contours in Figure 10, which shows that the flow has minimum cross-sectional area at about 0.5D downstream of pipe contraction, D being the diameter of the smaller pipe. Then, the pressure gradually increases and, after reaching its maximum, it merges into the curve of the pipe frictional pressure drop downstream of contraction. This local minimum value of pressure corresponds to the vena-contracta position. So, it can be concluded

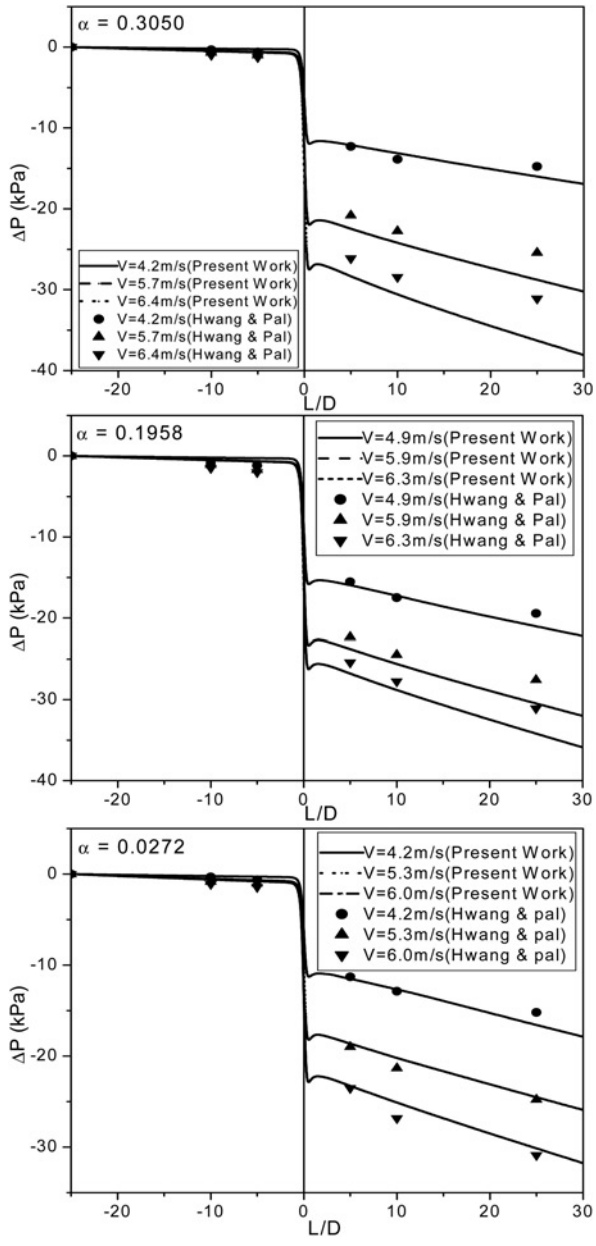

Figure 8.
Pressure profile for water-in-oil emulsion flowing through sudden contraction

that vena-contracta is always obtained in the two-phase flow of oil–water emulsions through sudden contraction at a distance of 0.5D from the contraction plane in the downstream direction. Simulated velocity vectors are shown in Figure 11, which clearly shows that eddy zones are formed in the separated flow region.

Figures 12 and 13 show the plot of $\Delta P_c/\rho$ vs the velocity head ($V^2/2$) for various differently concentrated oil-in-water and water-in-oil emulsions, respectively. It can be

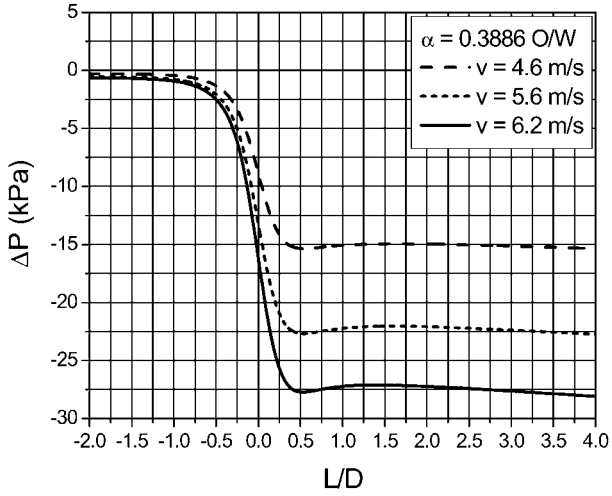

Figure 9.
Enlarged view of Figure 5 ($\alpha = 0.3886$) to check the occurrence and position of vena-contracta

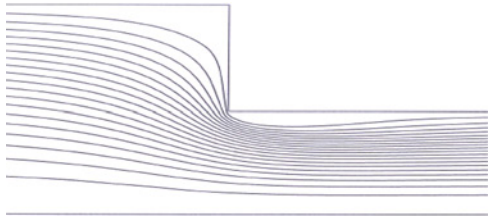

Figure 10.
Stream lines for $\alpha = 0.2124$ and v = 3.4 m/s

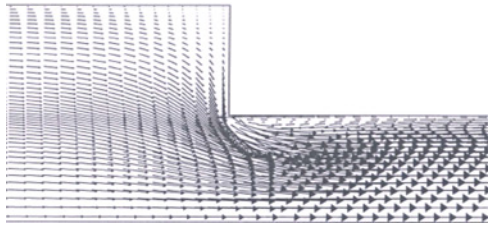

Figure 11.
Velocity vectors for $\alpha = 0.2124$ and v = 3.4 m/s

seen that $\Delta P_c/\rho$ vs $V^2/2$ data exhibit a linear relationship. K_2 is the slope of $\Delta P_c/\rho$ vs $V^2/2$ plots. Thus, the loss coefficient for contraction K_c is calculated for various differently concentrated oil-in-water and water-in-oil emulsions by using Equation (28). Here, K_1 is equal to$[(D_2/D_1)^4 - 1]$.

The plot of contraction loss coefficient (K_c) as a function of oil concentration is shown in Figure 14 for both emulsion types. It is observed that the loss coefficient is independent of oil concentration and has an average value of 0.537. The value of K_c calculated from the empirical equation, given in McCabe *et al.* (1993):

$$K_c = 0.4(1 - \beta) \tag{31}$$

is 0.302 for an area ratio (β) of about 0.244. The value obtained from Perry *et al.* (1984) is 0.43. The experimental value of K_c obtained by Hwang and Pal (1997) is 0.54. The

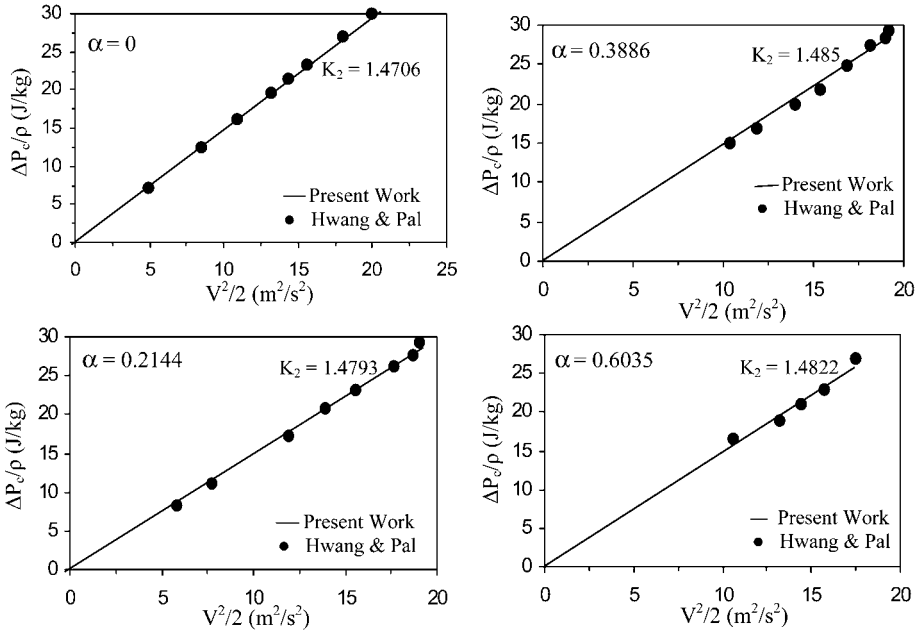

Figure 12.
$\Delta P_c/\rho$ vs $V^2/2$ data for oil-in-water emulsions flowing through a sudden contraction

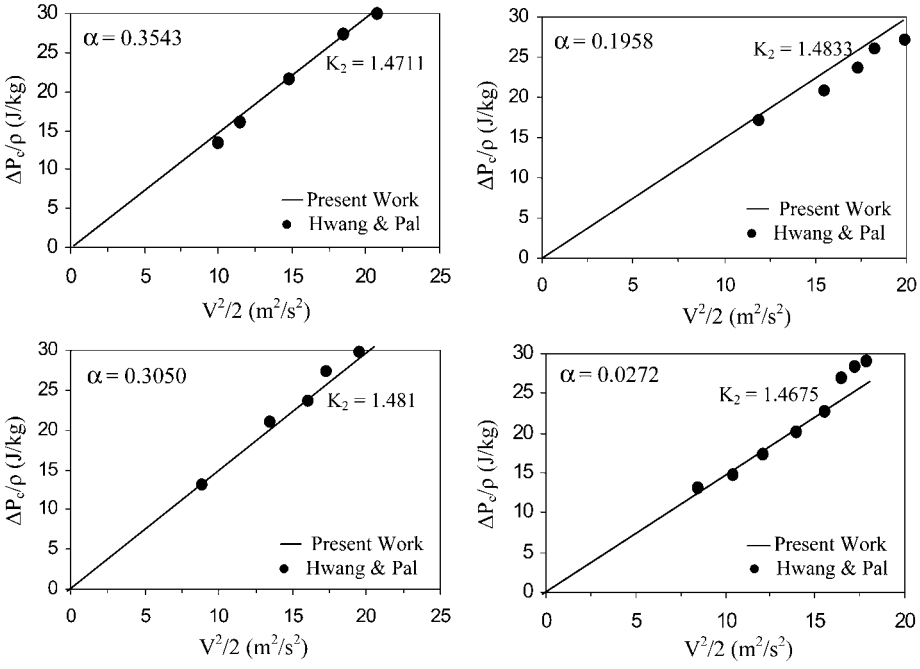

Figure 13.
$\Delta P_c/\rho$ vs $V^2/2$ data for water-in-oil emulsions flowing through a sudden contraction

presently computed loss coefficient can be used simply to compute the head loss across a sudden contraction in two-phase oil–water emulsions.

5.2 Sudden expansion

Computed as well as experimental pressure profiles for oil-in-water and water-in-oil emulsions at various fluid velocities are shown in Figures 15 and 16, respectively. The matching between the computation and that of the experimental observation for the pressure drop seems to be pretty reasonable in all these cases. It can be observed that the frictional loss in the inlet section causes the decline in pressure. As the fluid reaches the transitional section, the fluid is decelerated in the enlarged pipe area and there occurs a sudden rise in pressure. The pressure change at the expansion plane (ΔP_e) is

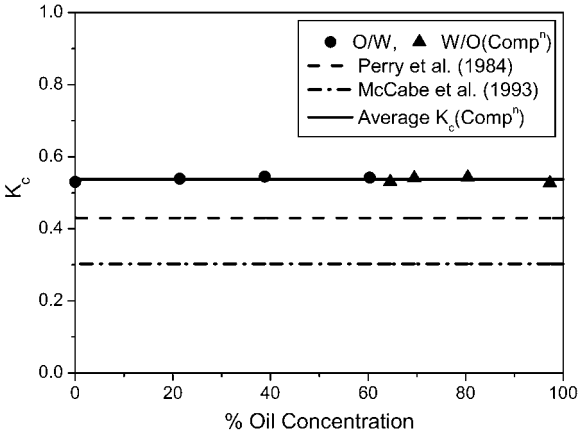

Figure 14.
Contraction loss coefficient as a function of oil concentration

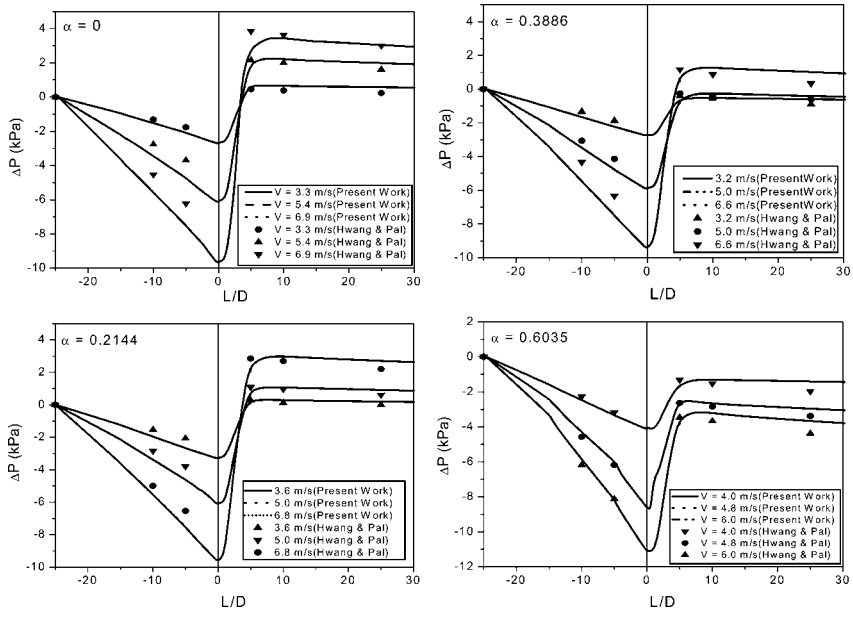

Figure 15.
Pressure profiles for oil-in-water emulsions flowing through a sudden expansion

obtained by extrapolating the computed pressure profiles upstream and downstream of the pipe expansion (in the region of fully developed pipe flow) to the expansion plane.

The streamlines and velocity vectors for $\alpha = 0.2144$ and $v = 6.8$ m/s are depicted in Figures 17 and 18, respectively. The streamlines take a typical diverging pattern and a zone of recirculating flow with turbulent eddies near the wall of the larger pipe are created in the corner. This is due to the fact that the fluid particles near the wall due to

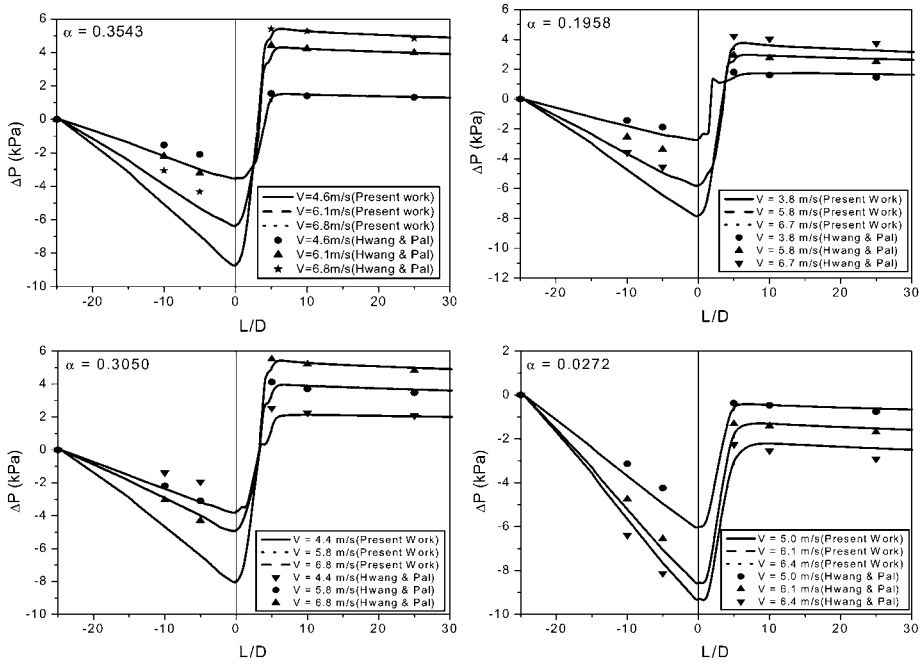

Figure 16.
Pressure profiles for water-in-oil emulsions flowing through a sudden expansion

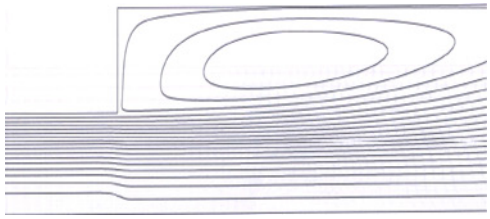

Figure 17.
Stream lines for $\alpha = 0.2144$ and $v = 6.8$ m/s

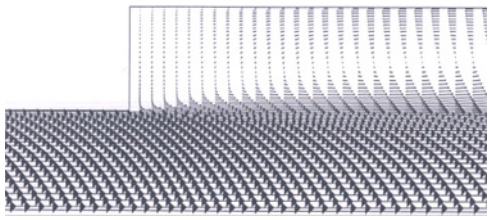

Figure 18.
Velocity vectors for $\alpha = 0.2144$ and $v = 6.8$ m/s

their low kinetic energy cannot overcome the adverse pressure hill in the direction of flow and hence follow up the reverse path under the favourable pressure gradient (since upstream pressure is lower than the downstream pressure as depicted in Figures 15 and 16).

Figures 19 and 20 show plot of $\Delta P_e/\rho$ vs velocity head $(V^2/2)$ for various differently concentrated oil-in-water and water-in-oil emulsions, respectively. It can be seen that $\Delta P_e/\rho$ vs $V^2/2$ data exhibit a linear relationship. K_2 is the slope of $\Delta P_e/\rho$ vs $V^2/2$ plots. Thus, the loss coefficient for expansion K_e which is equal to $(K_1 + K_2)$ is calculated for various differently concentrated oil-in-water and water-in-oil emulsions. Here $K_1 = [1 - (D_1/D_2)^4]$.

The K_e values for different emulsions are plotted as a function of oil concentration in Figure 21. Clearly, the expansion loss coefficient is found to be independent of oil concentration and has an average value of 0.432. The computed K_e values for emulsions are compared with the values obtained from the following equations:

- Borda–Carnot equation (Perry *et al.*, 1984):

$$K_e = (1 - \beta)^2 \tag{32}$$

- Equation of Wadle (1989):

$$K_e = 2\beta(1 - \beta) \tag{33}$$

where β is the ratio of the cross-sectional area of small pipe to that of large pipe. The β value for the expansion in the present work is 0.244. So the value of K_e obtained from Equations 32 and 33 are 0.5715 and 0.3689, respectively. The experimental value of K_e

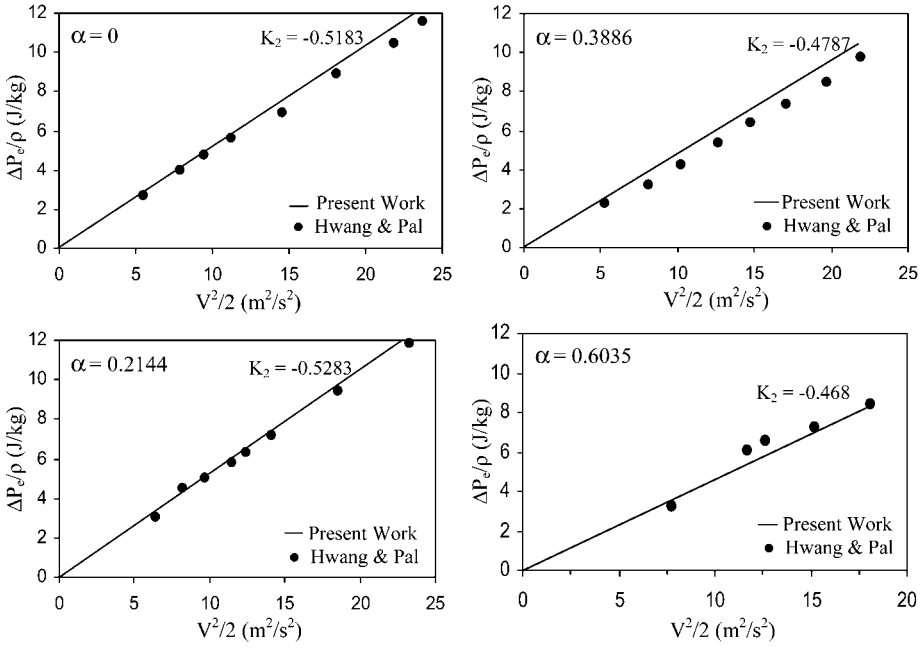

Figure 19.
$\Delta P_e/\rho$ vs $V^2/2$ for oil-in-water emulsions flowing through a sudden expansion

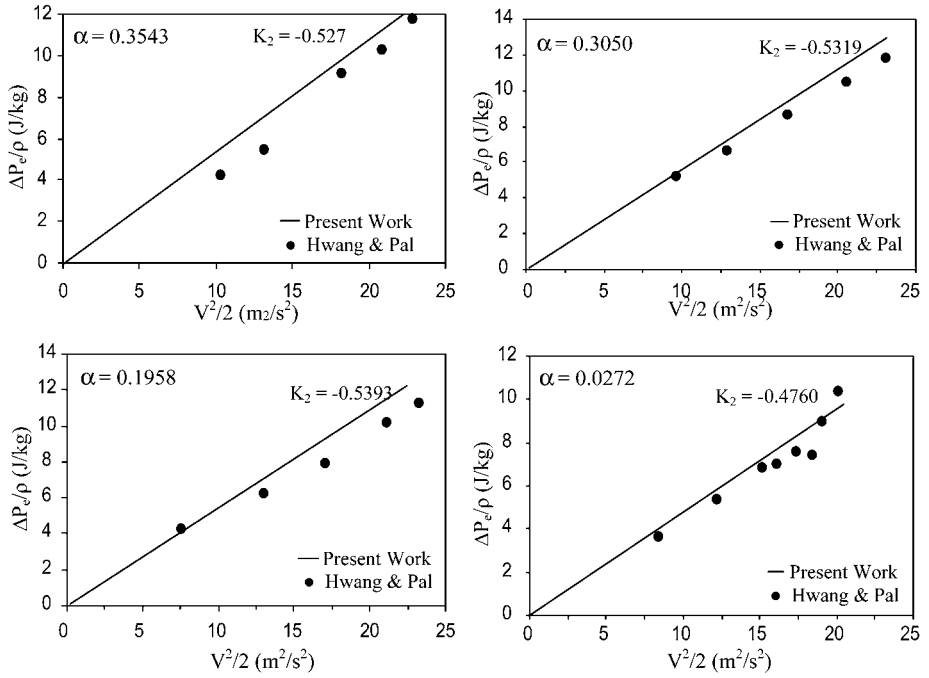

Figure 20.
$\Delta P_e/\rho$ vs $V^2/2$ data for water-in-oil emulsions flowing through a sudden expansion

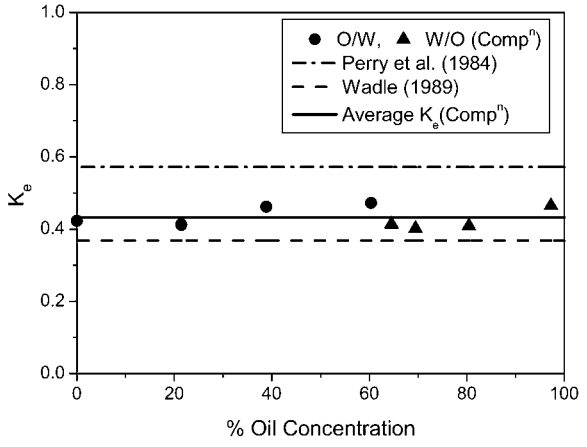

Figure 21.
Expansion loss coefficient as a function of oil concentration

obtained by Hwang and Pal (1997) is 0.47. As shown in Figure 21, the computed K_e values for all emulsions lie in between the two values obtained from Equations (32) and (33).

6. Conclusions

The flow through sudden contraction and expansion has been numerically investigated with oil–water emulsions by using two-phase flow model in an Eulerian scheme in this study. The major observations made relating to the pressure drop in the

process of flow through sudden expansion and contraction can be summarized as follows:

- The contraction/expansion loss coefficient is found to be independent of the velocity and hence Reynolds number.
- The loss coefficient is not significantly influenced by the type and concentration of oil–water emulsions flowing through sudden contraction and expansion.
- Effect of viscosity is negligible on the pressure drop through sudden contraction and expansion.
- The computed contraction loss coefficient is found to be slightly more than the predictions of Perry *et al.* (1984). Where as the McCabe *et al.* (1993) correlation under predicts the data significantly.
- The computed expansion loss coefficient is found to lie in between the two values obtained from Borda–Carnot equation (Perry *et al.*, 1984) and equation of Wadle (1989). It is in relatively close agreement with the predictions of Wadle (1989).
- The pressure drop increases with higher inlet velocity and hence with higher mass flow rate.
- In the single phase flow of water and two-phase flow of oil–water emulsions vena-contracta is always established at a distance of about 0.5D after the contraction section and depends only slightly on the concentration and velocity of flow.
- The satisfactory agreement between the numerical and experimental results indicates that the model may be used as a simple, efficient tool for engineering analysis of two-phase flow through sudden flow area expansions and contractions.

References

Abdelall, F.F., Hann, G., Ghiaasiaan, S.M., Abdel-Khalik, S.I., Jeter, S.S., Yoda, M. and Sadowski, D.L. (2005), "Pressure drop caused by abrupt flow area changes in small channels", *Experimental Thermal and Fluid Science*, Vol. 29, pp. 425-34.

Acrivos, A. and Schrader, M.L. (1982), "Steady flow in a sudden expansion at high Reynolds numbers", *Physics of Fluids*, Vol. 25 No. 6, pp. 923-30

Al'Ferov, N.S. and Shul'Zhenko, Ye N. (1977), "Pressure drops in two-phase flows through local resistances", *Fluid Mechanics – Soviet Research*, Vol. 6, pp. 20-33.

Aloui, F. and Souhar, M. (1996a), "Experimental study of a two-phase bubbly flow in a flat duct symmetric sudden expansion – part I: visualization, pressure and void fraction", *International Journal of Multiphase Flow*, Vol. 22 No. 4, pp. 651-65.

Aloui, F. and Souhar, M. (1996b), "Experimental study of a two-phase bubbly flow in a flat duct symmetric sudden expansion – part II: liquid and bubble velocities, bubble sizes", *International Journal of Multiphase Flow*, Vol. 22 No. 5, pp. 849-61.

Anglart, H., Nylund, O., Kurul, N. and Podowski, M.Z. (1997), "CFD prediction of flow and phase distribution in fuel assemblies with spacers", *Nuclear Engineering and Design*, Vol. 177, pp. 215-28.

Attou, A. and Bolle, L. (1995), "Evaluation of the two-phase pressure loss across singularities", *American Society Mechanical Engineers Fluids Engineering Division*, Vol. 210, pp. 121-7.

Attou, A., Giot, M. and Seynhaeven, J.M. (1997), "Modeling of steady-state two-phase bubbly flow through a sudden enlargement", *International Journal of Heat and Mass Transfer*, Vol. 40, pp. 3375-85.

Crowe, C., Sommerfeld, M. and Tsuji, Y. (1998), *Multiphase Flows with Droplets and Particles*, CRC Press, Boca Raton, FL.

Daniel, E. and Loraud, J.C. (1998), "Numerical simulation of a two-phase dilute flow in a diffuser pipe", *International Journal of Numerical Methods for Heat & Fluid Flow*, Vol. 8, No. 2, pp. 224-44.

Drew, D. and Lahey, R.T. Jr (1979), "Application of general constitutive principles to the derivation of multidimensional two-phase flow equations", *International Journal of Multiphase Flow*, Vol. 7, pp. 243-64.

Drew, D.A. (1983), "Mathematical modeling of two-phase flows", *Annual Revew of Fluid Mechanics*, Vol. 15, pp. 261-91.

Drew, D.A. and Passman, S.L. (1999), *Theory of Multicomponent Fluids*, Springer, New York, NY.

FLUENT User's Guide (2005), *Version 6.2.16*, Fluent Inc., Lebanon, NH.

Gidaspow, D. (1994), *Multiphase Flow and Fluidization: Continuum and Kinetic Theory Descriptions*, Academic Press, Boston, MA.

Gnglielmini, G., Lorenzi, A., Muzzio, A. and Sotgia, G. (1986), "Two-phase flow pressure drops across sudden area contractions pressure and void fraction profiles", *Proceeding of the 8th International Heat Transfer Conference*, Vol. 5, pp. 2361-6.

Hwang, C.Y.J. and Pal, R. (1997), "Flow of two phase oil/water mixtures through sudden expansions and contractions", *Chemical Engineering Journal*, Vol. 68, pp. 157-63.

Jansen, E. (1966), "Two-phase pressure loss across abrupt contractions and expansion, steam water mixtures at 600–1400 psia", *Int. Heat Transfer Conference ASME*, Vol. 5, pp. 13-25.

Kishan, P.A. and Dash, S.K. (2006), "Numerical and experimental study of circulation flow rate in a closed circuit due to gas jet impingement", *International Journal of Numerical Methods for Heat & Fluid Flow*, Vol. 16, No. 8, pp. 890-909.

Launder, B.E. and Spalding, D.B. (1974), "The numerical computation of turbulent flows", *Computer Methods in Applied Mechanics and Engineering*, Vol. 3, pp. 269-89.

McCabe, W.L., Smith, J.C. and Harriott, P. (1993), *Unit Operations of Chemical Engineering*, McGraw-Hill, New York, NY.

Mizushima, J. and Shiotani, Y. (2000), "Structural instability of the bifurcation diagram for two-dimensional flow in a channel with a sudden expansion", *Journal of Fluid Mechanics*, Vol. 420, pp. 131-45.

Pal, R. (1993), "Pipeline flow of unstable and surfactant-stabilized emulsions", *AIChE Journal*, Vol. 39 No. 11, pp. 1754-64.

Patankar, S.V. (1980), *Numerical Heat Transfer and Fluid Flow*, Hemisphere, Washington, DC.

Perry, R.H., Green, D.W. and Maloney, J.O. (1984), *Perry's Chemical Engineers' Handbook*, McGraw-Hill, New York, NY.

Ranade, V.V. (2002), *Computational Flow Modeling for Chemical Reactor Engineering*, Academic Press, London.

Salcudean, M., Groeneveld, D.C. and Leung, L. (1983), "Effect of flow obstruction geometry on pressure drops in horizontal air-water flow", *International Journal of Multiphase Flow*, Vol. 9 No. 1, pp. 73-85.

Schmidt, J. and Friedel, L. (1997), "Two-phase pressure drop across sudden contractions in duct areas", *International Journal of Multiphase Flow*, Vol. 23, pp. 283-99.

Shih, T.-H., Liou, W.W., Shabbir, A., Yang, Z. and Zhu, J. (1995), "A new $\kappa - \varepsilon$ eddy -viscosity model for high Reynolds number turbulent flows – model development and validation", *Computers Fluids*, Vol. 24 No. 3, pp. 227-38.

Tapucu, A., Teyssedou, A., Troche, N. and Merilo, M. (1989), "Pressure losses caused by area changes in a single channel flow under two-phase flow conditions", *International Journal of Multiphase Flow*, Vol. 15 No. 1, pp. 51-64.

Troshko, A.A. and Hassan, Y.A. (2001), "A two-equation turbulence model of turbulent bubbly flows", *International Journal of Multiphase Flow*, Vol. 27, pp. 1965-2000.

Vasquez, S.A. and Ivanov, V.A. (2000), "A phase coupled method for solving multiphase problems on unstructured meshes", *Proceedings of the ASME Fluids Engineering Division Summer Meeting (FEDSM2000)*, FED (American Society of Mechanical Engineers), Vol. 251, pp. 659-64.

Wadle, M. (1989), "A new formula for the pressure recovery in an abrupt diffuser", *International Journal of Multiphase Flow*, Vol. 15 No. 2, pp. 241-56.

Wallis, G.B. (1969), *One-Dimensional Two-Phase Flow*, McGraw-Hill, New York, NY.

Further reading

Brennen, C.E. (2005), *Fundamentals of Multiphase Flow*, Cambridge University Press, New York, NY.

Ezzeddine, H.T. and Taieb, L. (1998), "Transient flow of homogeneous gas-liquid mixtures in pipelines", *International Journal of Numerical Methods for Heat & Fluid Flow*, Vol. 8 No. 3, pp. 350-68.

Ishii, M. and Zuber, N. (1979), "Drag coefficient and relative velocity in bubbly, droplet or particulate flows", *AIChE Journal*, Vol. 25, pp. 843-55.

Jha, P.K. and Dash, S.K. (2004), "Employment of different turbulence models to the design of optimum steel flows in a tundish", *International Journal of Numerical Methods for Heat & Fluid Flow*, Vol. 14 No. 8, pp. 953-79

Launder, B.E. and Spalding, D.B. (1972), *Lectures in Mathematical Models of Turbulence*, Academic Press, London.

Sebahattin, U., Selahaddin, O.A. and Ahmet, K. (2007), "Investigation of heat transfer and pressure drop for various obstacles in a rectangular-sectioned 90° bend", *International Journal of Numerical Methods for Heat & Fluid Flow*, Vol. 17 No. 5, pp. 494-11.

Corresponding author

Sukanta K. Dash can be contacted at: sdash@mech.iitkgp.ernet.in